Journal of Applied Polymer Science

Fe_3O_4/poly(acrylic acid) hybrid nanoparticles for water-based drilling fluids

Yuanpeng Wu,[1,2] Zhu Yan,[1] Pingquan Wang,[2] Pingya Luo,[2] Yuanhua Lin[1,2]

[1]Center of New Energy Materials and Technology, School of Materials Science and Engineering, Southwest Petroleum University, Chengdu, Sichuan Province 610500, People's Republic of China

[2]State Key Laboratory of Oil and Gas Reservoir Geology and Exploitation, Southwest Petroleum University, Chengdu, Sichuan Province 610500, People's Republic of China

Correspondence to: Y. Wu (E-mail: ypwu@swpu.edu.cn)

ABSTRACT: Because of the sizes of the pore throat are on the nanometer scale, nanoparticles with sizes on the nanoscale have been developed as candidates for plugging materials during drilling in shale formation. In this study, Fe_3O_4 nanoparticles were prepared by a coprecipitation method, and then, Fe_3O_4/poly(acrylic acid) (PAA) hybrid nanoparticles were obtained through the modification of the Fe_3O_4 nanoparticles with PAA. The hybrid nanoparticles were characterized by Fourier transform infrared spectroscopy, transmission electron microscopy, and thermogravimetric analysis. The magnetic properties, salt tolerance, and compatibility with sulfomethylated phenolic resin of the nanoparticles were studied. The plugging properties of the Fe_3O_4/PAA hybrid nanoparticles were evaluated by filtration testing of the filter cakes at ambient temperature and 80 °C. © 2016 Wiley Periodicals, Inc. J. Appl. Polym. Sci. **2016**, *133*, 44010.

KEYWORDS: magnetism and magnetic properties; nanoparticles; poly(acrylic acid)

Received 14 February 2016; accepted 2 June 2016

DOI: 10.1002/app.44010

INTRODUCTION

With increasing depletion of conventional energy resources, the development of unconventional energy resources, such as shale gas, shale oil, and tight sandstone gas, have attracted more attention. However, the formation structures of reservoirs of shale gas, shale oil, and tight sandstone gas are very complex,[1,2] and the drilling process may present many difficult problems.[3] One of the key issues is the fact that during drilling in shale formation, conventional plugging materials are not effective because the size of the holes in shale formation is smaller than that in other formations. The size of these holes is probably on the nanometer scale. For better plugging performance during drilling in shale formations, smaller and more effective plugging materials for use in water-based drilling fluids are needed.

Nanotechnology has been widely used in many areas, including the electronics industry, the paints and coatings industry, biomaterials, medical materials, energy materials, and cosmetic materials.[4] The application of nanotechnology in the oil and gas industry and related areas is relatively new. Recently, because of their unique properties, nanoparticles have been added to drilling fluids to improve their performance.[5,6] Nanoparticles with sizes from 1 to 100 nanometers exhibit excellent potential as plugging materials of water-based drilling fluids used in shale formations.[7] Typically, 3- and 30-nm Fe_2O_3 nanoparticles are added to water-based drilling fluids to decrease fluid loss through the blocking of micropores and nanopores in filter cakes.[8] However, these magnetic nanoparticles can aggregate easily in water-based fluids, and this results in bigger particles and leads to higher fluid losses.[9,10] Because pure inorganic nanoparticles are prone to aggregation because of their high surface energy, for practical applications, nanoparticles in drilling fluids should be well dispersed, even at high temperatures and in high salt conditions during formation. To improve the dispersed stability of magnetic nanoparticles in water-based fluids and to decrease their fluid loss, a negatively charged polyelectrolyte, that is, poly(acrylic acid) (PAA), was synthesized to modify nanoparticles, and the hybrid nanoparticles were added to water-based fluids to enhance their plugging performance.

In this study, Fe_3O_4 nanoparticles and PAA were first prepared by a coprecipitation method and solution polymerization, respectively. Then, the surfaces of the Fe_3O_4 nanoparticles were modified by PAA to produce Fe_3O_4/PAA hybrid nanoparticles. Their magnetic responsiveness, salt tolerance, and compatibility with polymeric additives were examined. The plugging properties of the Fe_3O_4/PAA nanoparticles were investigated via filtration tests on filter cakes at ambient temperature and 80 °C.

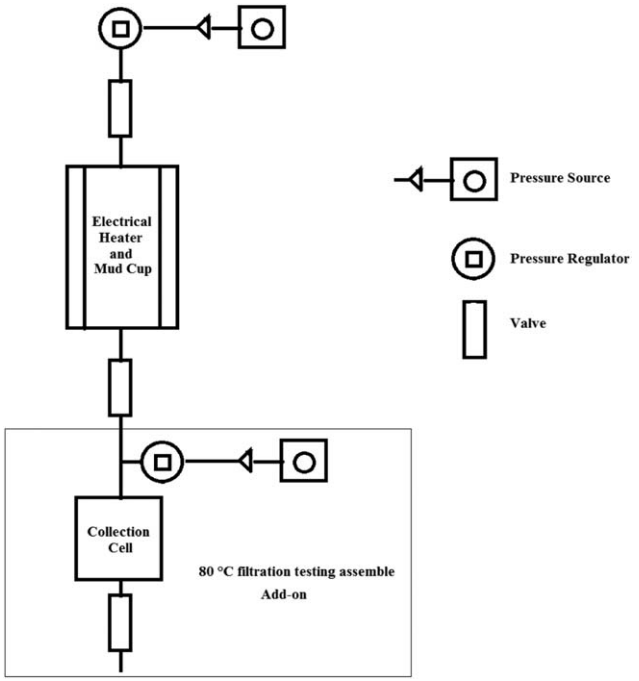

Scheme 1. Illustration of the filtration testing and formation of filter cakes.

EXPERIMENTAL

Materials

Ferric chloride hexahydrate ($FeCl_3 \cdot 6H_2O$), ferrous sulfate heptahydrate ($FeSO_4 \cdot 7H_2O$), ammonia ($NH_3 \cdot H_2O$; 25%), acrylic acid (AA), potassium persulfate, sodium chloride (NaCl), and sulfomethylated phenolic resin (SMP) were purchased from Kelong Chemical Reagent Factory (Chengdu, China), and all of the reagents were analytical grade.

Synthesis

Preparation of Magnetic Fe_3O_4 Nanoparticles. Fe_3O_4 nanoparticles were prepared by a coprecipitation method.[11] $FeCl_3 \cdot 6H_2O$ (1.4 g) and $FeSO_4 \cdot 7H_2O$ (0.85 g) were dissolved in distilled water under mechanical stirring. Then, $NH_3 \cdot H_2O$ (20 mL) was added and reacted for 2 h at 40 °C. Fe_3O_4 nanoparticles were separated and washed with distilled water several times with the assistance of a magnet and dried at 60 °C for 24 h *in vacuo*.

Preparation of PAA by Solution Polymerization. PAA was prepared by the solution polymerization of AA. In a typical procedure, AA (6.5 g) and potassium persulfate (0.08 g) were dissolved in distilled water and reacted at 80 °C for 12 h. Then, the solution was dialyzed against distilled water for a week. We obtained PAA by evaporating the water.

Preparation of Magnetic Fe_3O_4/PAA Hybrid Nanoparticles. Fe_3O_4 (0.5 g) was dissolved in 80 mL of distilled water and slowly dropped into a 60-mL aqueous solution of PAA (5 g) under mechanical stirring. The mixture was reacted at ambient temperature for 4 h, separated, and washed with distilled water several times with the assistance of a magnet. We obtained the Fe_3O_4/PAA hybrid nanoparticles by vacuum drying the mixture at 60 °C for 24 h.

Characterization

Instrumentation and Characterization. Fourier transform infrared (FTIR) spectra were acquired with a Nicolet 6700 FTIR spectrometer. Transmission electron microscopy (TEM) images were obtained with an H-600 transmission electron microscope. The samples were prepared by the placement of a drop of the nanoparticle solution sample on a copper grid. Thermogravimetric analysis (TGA) was conducted in nitrogen on a TGA/SDTA85 thermal analyzer at a scanning rate of 10 °C/min. Plugging properties tests were conducted with a GGS42-2 high-temperature, high-pressure filtration press.

Salt Tolerance of the Fe_3O_4/PAA Hybrid Nanoparticles. The Fe_3O_4/PAA dispersion stability analysis was conducted by the measurement of the stable time in an NaCl aqueous solution. In a typical procedure, we mixed stock solutions of NaCl and the Fe_3O_4/PAA dispersion samples to reach desired NaCl concentrations of 0, 0.1, 0.2, 0.4, 0.5, 0.8, 1, 2, 4, 5, 7, and 10 wt % and a desired Fe_3O_4/PAA concentration of 0.6 wt %. The coagulation behaviors of the dispersions were observed, and the stable time of each solution was recorded.

Compatibility Properties of the Fe_3O_4/PAA Hybrid Nanoparticles with SMP. Fe_3O_4/PAA hybrid nanoparticles were dispersed in an SMP aqueous solution to reach concentrations of 1, 2, and 3 wt % SMP and 0.6 wt % Fe_3O_4/PAA. Then, these dispersions were kept in an oven at different temperatures for 10 h, and the coagulation behaviors of the dispersions were recorded. The test temperatures were from 80 to 220 °C with an increasing gradient of 10 °C.

Filtration Test. The plugging performance of the Fe_3O_4/PAA nanoparticles was tested through the filtration of a water solution containing nanoparticles on the filter cakes. The filter cakes were formed by the dissolution of 120 g of barite in 100 mL of water and filtration on a high-temperature and high-pressure filter press with an area of 22.6 cm^2 and a pressure difference of 3.5 MPa (Scheme 1). Then, the fluid loss of water in the samples containing 0.8, 1.6, and 2.4 wt % Fe_3O_4/PAA hybrid nanoparticles were tested on the filter cake at room temperature and 80 °C. The volumes of fluid loss were recorded per minute, and then, the permeabilities of the filter cake before and after plugging with nanoparticles were calculated by Darcy's law from the total filtrate volumes at 30 min.

RESULTS AND DISCUSSION

Synthesis of the PAA and Fe_3O_4/PAA Nanoparticles

PAA was synthesized through free-radical solution polymerization and modified on the surface of Fe_3O_4 nanoparticles, which were prepared by the coprecipitation method, to fabricate the Fe_3O_4/PAA hybrid nanoparticles (Scheme 2).

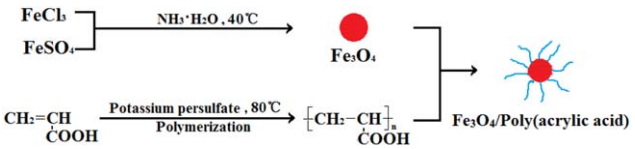

Scheme 2. Fabrication of the Fe_3O_4/PAA hybrid nanoparticles. [Color figure can be viewed in the online issue, which is available at wileyonlinelibrary.com.]

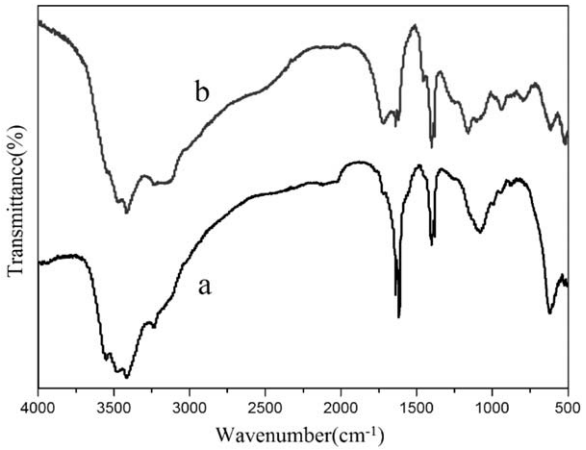

Figure 1. FTIR spectra of (a) Fe_3O_4/PAA and (b) PAA.

Figure 1 gives the FTIR spectra of PAA and Fe_3O_4/PAA. As shown in Figure 1(a), the peak at 623 cm^{-1} was attributed to the stretching vibrations of Fe—O—Fe. The peaks at 3420, 1630, 1460, and 1160 cm^{-1} were attributed to stretching vibrations of the hydroxyl group, stretching vibrations of the carbonyl group, scissor vibrations of the $—CH_2$ group, and stretching vibrations of the —C—O group, respectively. These peaks were consistent with the peaks of PAA, as shown in Figure 1(b), and indicated that PAA was modified on the surface of the Fe_3O_4 nanoparticles and hybrid nanoparticles were formed.

Morphology and Thermal Stability of the Fe_3O_4/PAA Hybrid Nanoparticles

The TEM image and TGA curve of the as-synthesized Fe_3O_4/PAA hybrid nanoparticles are shown in Figure 2. As shown in Figure 2(a), the morphology of the hybrid nanoparticles was a uniform sphere with an average size of 20 nm. The hybrid nanoparticles were dispersed well in the aqueous solution.

Figure 2(b) shows the TGA curve of the hybrid nanoparticles. Fe_3O_4/PAA exhibited two weight loss stages. The first weight loss process (ca. 2 wt %), from room temperature to 130 °C, was attributed to the release of free adsorbed water. The second weight loss process (ca. 13 wt %), in the range 220–450 °C, was due to the decomposition of PAA chains linking on the surface

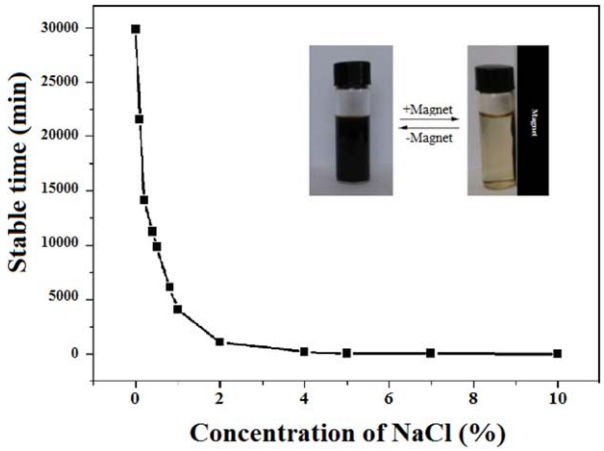

Figure 3. Salt tolerance and magnetic responsiveness of the Fe_3O_4/PAA hybrid nanoparticles in water. [Color figure can be viewed in the online issue, which is available at wileyonlinelibrary.com.]

of the hybrid nanoparticles. These results confirmed that PAA was successfully modified on the Fe_3O_4 nanoparticles, and the polymers in the composites had a concentration of 13.3 wt %.

Salt Tolerance and Magnetic Properties of the Fe_3O_4/PAA Hybrid Nanoparticles

For practical applications, the dispersed stability of magnetic nanoparticles in salty water should be taken into consideration because many kinds of salts can dissolve in water-based drilling fluids when drilling is performed in shale formations. The dispersed stability of Fe_3O_4/PAA nanoparticles was characterized in an NaCl aqueous solution. The stable times of the Fe_3O_4/PAA dispersion with different NaCl concentrations are shown in Figure 3. The stable time of the Fe_3O_4/PAA hybrid nanoparticles without NaCl was as long as about 21 days. When the concentration of NaCl was increased, the stable times of the dispersion decreased to about 15 days at 0.1 wt % and about 3.5 h at 4 wt %, respectively. The stable time sharply decreased to 26 min when the concentration of NaCl increased to 5 wt %, and a further increase in the NaCl concentration did not cause a remarkable reduction in the stable time. These results indicate that the Fe_3O_4/PAA hybrid nanoparticle dispersion was stable when the

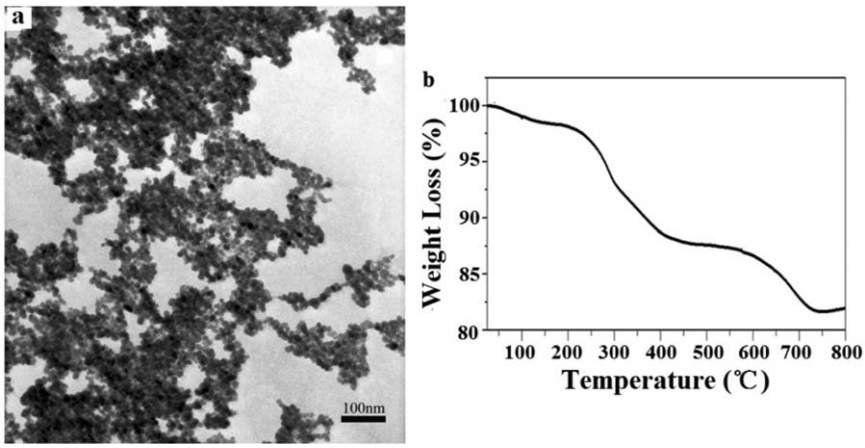

Figure 2. (a) TEM image and (b) TGA curve of the Fe_3O_4/PAA hybrid nanoparticles.

Table I. Compatibility of the Fe_3O_4/PAA Nanoparticles with SMP at Different Concentrations and Temperatures

SMP (wt %)	Temperature (°C)														
	80	90	100	110	120	130	140	150	160	170	180	190	200	210	220
1	U	U	U	U	U	U	U	U	U	U	U	U	D	D	D
2	U	U	U	U	U	U	U	U	U	U	U	U	D	D	D
3	U	U	U	U	U	U	U	U	U	U	U	U	D	D	D

D, deposited; U, undeposited.

NaCl concentration was below 5 wt %. Therefore, they could fit the requirements of drilling applications in many kinds of shale formations.

The magnetic responsiveness of the hybrid nanoparticles was examined with an exterior magnet. When a magnet was put on one side of the aqueous dispersion of the hybrid nanoparticles, the nanoparticles were completely adsorbed to the side near the magnet within 5 min. The hybrid nanoparticles could be redispersed into the aqueous solution by gentle shaking after the magnet was removed. This reversible process could be repeated many times without any precipitation of the nanoparticles. These results indicate that the hybrid nanoparticles exhibited good responsiveness to a magnetic field and could be move to a target region in formation. This property gives the as-prepared Fe_3O_4/PAA nanoparticles great advantages for recycling and reuse.

Compatibility of the Fe_3O_4/PAA Hybrid Nanoparticles

Usually, there are additives in water-based drilling fluids, including SMP and other polymers. So, the compatibility of the Fe_3O_4/PAA nanoparticles with these additives needed to be taken into account. As shown in Table I, when the concentration of SMP was increased from 1 to 3 wt %, the dispersions of the hybrid nanoparticles were stable from 80 to 190 °C. The hybrid nanoparticles deposited from the solution when the temperature was increased above 200 °C. These results indicate that the Fe_3O_4/PAA hybrid nanoparticles show excellent compatibility with SMP until the temperature of the water-based fluids was elevated to 190 °C.

Plugging Properties of the Fe_3O_4/PAA Hybrid Nanoparticles

In this study, man-made filter cakes were used to simulate shale formation. When an aqueous solution containing nanoparticles flowed through the man-made filter cakes, the pores in the cakes were blocked (Scheme 3). This process was performed just as water-based drilling fluids containing plugging materials are used in shale formation.

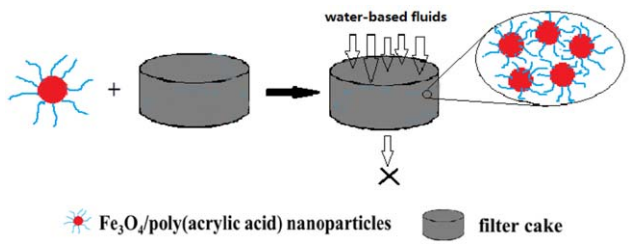

Scheme 3. Illustration of the Fe_3O_4/PAA nanoparticles in water-based fluids blocking the pores in the filter cakes. [Color figure can be viewed in the online issue, which is available at wileyonlinelibrary.com.]

Once these pores were plugged by nanoparticles, the filtration of these kinds of fluids decreased. The filtration of water and water containing different nanoparticle fractions at room temperature and 80 °C is depicted in Figure 4. The fluid loss decreased obviously after the introduction of Fe_3O_4/PAA nanoparticles both at room temperature and 80 °C. The fluid loss of water on man-made filter cakes was 29.4 mL at 30 min at room temperature. With the addition of 0.8 wt % Fe_3O_4/PAA nanoparticles, the fluid loss decreased to 9.8 mL, with a reduction in the fluid filtrate volume of 66.7%. As shown in Figure 4(a), the fluid loss still continued to decrease with increasing amount of Fe_3O_4/PAA nanoparticles. When the amount of nanoparticles in the fluid was increased to 1.6 and 2.4 wt %, the fluid loss decreased to 5.6 and 5.1 mL, respectively. The corresponding reductions were 80.9 and 82.7%, respectively.

However, with an increase in the temperature from room temperature to 80 °C, the fluids containing nanoparticles also exhibited an obvious decrease in fluid loss in comparison to the water control [Figure 4(b)]. Fluids without nanoparticles exhibited a fluid loss equal to 35.3 mL at 30 min and 80 °C. When the Fe_3O_4/PAA nanoparticle concentrations were increased to 0.8, 1.6, and 2.4 wt %, the fluid losses of these nanoparticles fluids decreased to 9.2, 5.5, and 4.8 mL, respectively. So, the reductions of filtration were 73.9, 84.4, and 87.3%. These decreased fluid losses of fluids containing nanoparticles demonstrated that nanoparticles are important for water-based drilling fluids used in water-sensitive formations, especially in shale formations.

The plugging properties of nanoparticles in filter cakes can vary with permeability. The permeabilities of the filter cakes before and after plugging with nanoparticles were calculated with Darcy's law[8] from the fluid loss of these fluids. Darcy's law is expressed as follows:

$$\frac{dV}{dt} = \frac{KA\Delta p}{\mu h}$$

The law describes the fluid filtrate volume (dV) as a function of time (dt). A is the cross-sectional area, K is the permeability, Δp is the pressure differential, μ is the viscosity, and h is the thickness of the filter cakes.

The permeability of the filter cake before plugging by nanoparticles was calculated to be 0.000413 μm^2 from Darcy's law, whereas the permeabilities of the filter cakes plugged with

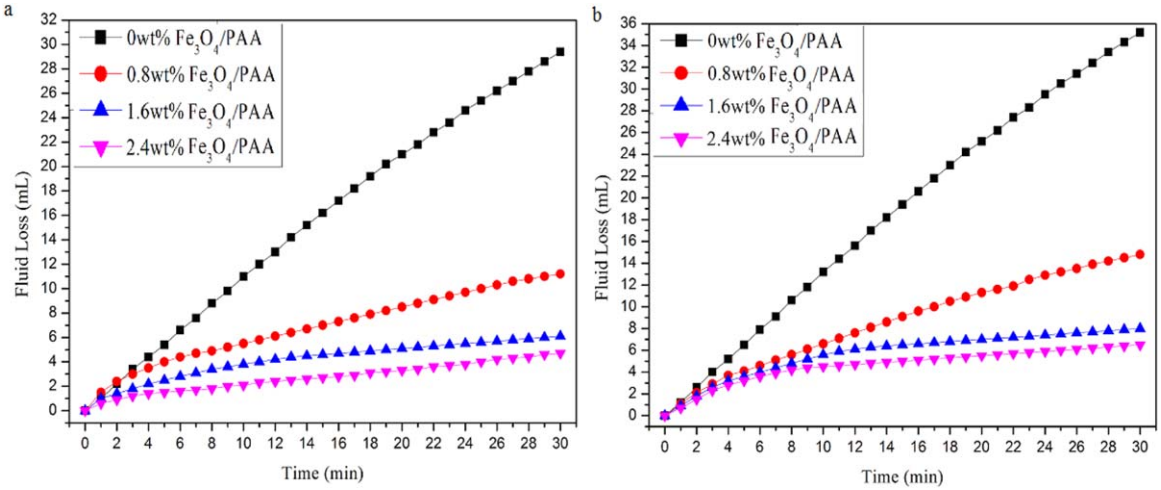

Figure 4. Fluid losses of water-based fluids with and without Fe_3O_4/PAA nanoparticles versus time at (a) room temperature and (b) 80 °C. [Color figure can be viewed in the online issue, which is available at wileyonlinelibrary.com.]

Fe_3O_4/PAA hybrid nanoparticles under different conditions are provided in Table II.

When water fluids with nanoparticles flowed though the man-made filter cakes, the cakes were plugged by the nanoparticles, and thus, the fluid loss and permeability decreased. According to Table II, the plugging of the filter cakes with 0.8, 1.6, and 2.4 wt % Fe_3O_4/PAA nanoparticle dispersions at room temperature led to 66.6, 81.1, and 82.6% reductions, respectively, in the permeability compared to the pure water control. When fluids containing nanoparticles flowed through filter cakes, the Fe_3O_4/PAA nanoparticles were squeezed into the micropores or cracks of the filter cake under a high differential pressure (3.5 MPa), and this led to physical blocking.[12–14] The permeability of the filter cakes plugged by nanoparticles decreased because of the reduced pore sizes; this was attributed to the fact that the empty spaces in the filter cakes were occupied by Fe_3O_4/PAA hybrid nanoparticles and these blocked the small pores and led to low permeability values and fluid filtrate volumes. The number of Fe_3O_4/PAA hybrid nanoparticles squeezed into the filter cakes increased when the concentration of Fe_3O_4/PAA in the water fluids was increased; this yielded a compact structure and a low porosity in the filter cakes and prevented filtration.[15,16]

The as-prepared Fe_3O_4/PAA nanoparticles showed a similar filtration decrease at 80 °C; this indicated that the Fe_3O_4/PAA nanoparticles retained an efficient plugging performance at high temperature. This was attributed to the dispersion stability of the Fe_3O_4/PAA nanoparticles in water, and thus, tight filter cakes were formed. The dissociation of PAA chains modified on the surface of the Fe_3O_4 nanoparticles induced negative charges on the surface of the nanoparticles and led to electrostatic repulsion between the nanoparticles.[17,18] The repulsion of the PAA layer greatly improved the stability of the Fe_3O_4/PAA by preventing nanoparticles from aggregating at 80 °C. The well-dispersed Fe_3O_4/PAA nanoparticles could be squeezed into the pores of the filter cakes under differential pressure and could be deformed to a suitable shape in the pores at high temperatures. Thus, more tight cakes were obtained, and this resulted in lower fluid loss and permeability at 80 °C.

CONCLUSIONS

Fe_3O_4/PAA hybrid nanoparticles were synthesized through a facile approach. TEM imaging showed that the sizes of these nanoparticles were about 20 nm. FTIR spectroscopy and TGA indicated that PAA was modified on the surface of the Fe_3O_4 nanoparticles and the weight fraction of PAA was nearly 13.3 wt %. These nanoparticles were magnetically responsive and could be easily controlled and moved to target places in shale formations with an exterior magnet. The nanoparticles were salt tolerant and could be dispersed stably in water-based drilling fluids with NaCl concentrations as high as 5 wt %. The nanoparticles were very compatible with SMP in the water fluids until temperature was increased to 190 °C. The incorporation of nanoparticles readily improved the fluid losses of the water-based drilling fluids. With the introduction of 2.4 wt % nanoparticles, the permeability decreased

Table II. Permeability of the Water-Based Fluids with Nanoparticles Calculated with Darcy's Law

	Fe_3O_4/PAA concentration			
	0 wt %	0.8 wt %	1.6 wt %	2.4 wt %
Room temperature				
V_{30} (mL)	29.4	9.8	5.6	5.1
Permeability (10^{-4} μm^2)	4.13	1.38	0.78	0.72
% change	—	−66.7	−80.9	−82.7
80 °C				
V_{30} (mL)	35.3	9.2	5.5	4.8
Permeability (10^{-4} μm^2)	4.96	1.29	0.77	0.67
% change	—	−68.8	−81.4	−83.8

V_{30}, volume of fluid loss from 0 to 30 min.

obviously to 82.7 and 83.8% at room temperature and 80 °C, respectively. These excellent performances showed that the Fe_3O_4/PAA nanoparticles are promising additives for water-based drilling fluids for drilling in shale formations.

ACKNOWLEDGMENTS

This work was financially supported by the National Natural Science Foundation of China (contract grant number 51304166), the Open Fund of the State Key Laboratory of Oil and Gas Reservoir Geology and Exploitation of Southwest Petroleum University (contract grant numbers PLN1112 and 1201), the China Postdoctoral Science Foundation (contract grant number 2014T70883), and the Foundation of the Science and Technology Bureau of Chengdu (contract grant number 12DXYB191JH-002).

REFERENCES

1. Gale, J. F. W.; Reed, R. M.; Holder, J. *AAPG Bull.* **2007**, *91*, 603.
2. Ross, D. J. K.; Bustin, R. M. *AAPG Bull.* **2008**, *92*, 87.
3. Wang, J. H.; Li, J. N.; Yan, L. L.; Ji, Y. H. *Adv. Mater. Res.* **2013**, *807*, 2602.
4. Sanchez, C.; Belleville, P.; Popall, M. *Chem. Soc. Rev.* **2011**, *40*, 696.
5. Sadeghalvaad, M.; Sabbaghi, S. *Powder Technol.* **2015**, *272*, 113.
6. Mohammadi, M.; Kouhi, M.; Sarrafi, A.; Schaffie, M. *Res. Chem. Intermed.* **2015**, *41*, 2823.
7. Mao, H.; Qiu, Z. S.; Shen, Z. H. *Prog. Nat. Sci. Mater.* **2015**, *25*, 90.
8. Barry, M. M.; Jung, Y. S.; Lee, J. K. *J. Pet. Sci. Eng.* **2015**, *127*, 338.
9. Son, Y. H.; Lee, J. K.; Soong, Y. *Chem. Mater.* **2010**, *22*, 2226.
10. Tombácz, E.; Czanaky, C.; Illés, E. *Colloid Polym. Sci.* **2001**, *279*, 484.
11. Chen, T. Y.; Cao, Z.; Guo, X. L.; Nie, J. *J. Polymer* **2011**, *52*, 172.
12. William, J. K. M.; Ponmani, S.; Samuel, R.; Nagarajan, R. *J. Pet. Sci. Eng.* **2014**, *117*, 15.
13. Ragab, A. M. S.; Noah, A. *Pet. Technol. Dev. J.* **2014**, *2*, 75.
14. Kasiralvalad, E. *Int. J. Nano Dimension* **2014**, *5*, 463.
15. Cheraghian, G.; Hemmati, M.; Bazgir, S. *AIP Conf. Proc.* **2014**, *1590*, 266.
16. Cai, J.; Chenevert, M. E.; Sharma, M. M.; Friedheim, J. *SPE Drill Completion* **2012**, *27*, 103.
17. Gonzatti, G. K.; Netz, P. A.; Fiel, L. A.; Pohlmann, A. R. *J. Braz. Chem. Soc.* **2015**, *26*, 373.
18. Booth, A.; Storseth, T.; Altin, D.; Fornara, A. *Sci. Total. Environ.* **2015**, *505*, 596.